Winter/summer mesopause temperature transition at Davis (69°S) in 2011/2012

F.-J. Lübken[1], J. Höffner[1], T. P. Viehl[1], B. Kaifler[2], and R. J. Morris[3]

[1]Leibniz-Institute of Atmospheric Physics, Kühlungsborn, Germany, [2]Institute of Physics of the Atmosphere, Wessling, Germany, [3]Australian Antarctic Division, Kingston, Tasmania, Australia

Abstract We present quasi-continuous measurements of temperature profiles in the Southern Hemisphere mesopause region during the transition from winter to summer conditions in 2011/2012. In a period of 120 days around solstice, we have performed iron lidar observations at Davis (69°S), Antarctica, for a total of 736 h. The winter/summer transition is identified by a downward shift of the mesopause which occurs on 8 November 2011. Soon after transition, mesopause heights and temperatures are similar to the Northern Hemisphere (NH) colatitude summer (88 km, 130 K). Around solstice, the mesopause is elevated for several days by 4–5 km and is colder than typical NH temperatures by 10 K. In this period individual profiles show temperatures as low as 100 K. The occurrence of polar mesosphere summer echoes is closely connected to low temperatures. Below 88 to 90 km and in the main summer season of 2011/2012 temperatures at Davis are generally warmer compared to the NH by 5–15 K, whereas temperatures are generally colder above 90 km. The winter/summer transition and the first appearance of polar mesosphere summer echoes are strongly correlated to maximum zonal winds in the stratosphere which constrain gravity waves with eastward momentum reaching the mesosphere. At the breakdown of the stratospheric vortex around solstice, the mesopause is higher and, surprisingly, colder than normal.

1. Introduction

The winter/summer transition in the mesosphere/lower thermosphere (MLT) region is substantially more variable in the Southern Hemisphere (SH) compared to its Northern Hemisphere (NH) counterpart, mainly due to altering stratospheric circulation changes impacting gravity wave forcing of the MLT [*Karlsson et al.*, 2007; *Smith et al.*, 2010]. Ice layers in the summer mesopause region require very low temperatures and have therefore been used as indirect indicators of the thermal conditions in the MLT. They have recently been studied with respect to circulation changes in the stratosphere [*Karlsson et al.*, 2011; *Benze et al.*, 2012]. Under summer conditions temperature measurements with sufficient temporal/spatial sampling and adequate accuracy are limited to few lidar observations and a couple of sounding rocket flights [*Pan and Gardner*, 2003; *Lübken et al.*, 2004; *Chu et al.*, 2011]. We have transported our mobile iron lidar to Davis, Antarctica, in late 2010 and performed measurements until the end of 2012. First results from the summer season 2010/2011 have been reported elsewhere [*Lübken et al.*, 2011; *Morris et al.*, 2012]. Although temperatures are available throughout the instrument operation period, here we present temperature measurements in the MLT region from spring equinox throughout the summer to examine the winter/summer transition 2011/2012 and to compare with circulation conditions in the stratosphere.

We compare our lidar temperatures with polar mesosphere summer echoes (PMSE) measured by the Australian Antarctic Division (AAD) 50 MHz VHF radar which is also located at Davis [*Morris et al.*, 2006]. PMSE are strong radar echoes in the summer mesopause region which are caused by fluctuations in electron densities at the radar Bragg scale ($\lambda/2 = 3$ m). These fluctuations rely on neutral air turbulence in combination with charged ice particles (see review by *Rapp and Lübken* [2004], and references therein). PMSE are therefore an indication of the presence of ice particles and low temperatures.

We would like to compare the winter/summer transition in 2011/2012 with the "normal" state of the SH summer mesopause region. Unfortunately, a reliable reference climatology based on observations is not available since measurements are sparse and do not cover the entire season or height. For example, the compilation published in *Pan and Gardner* [2003] relies on only 26 h of lidar observations in December–February (none in November) and hardly covers the mesopause. We therefore decided to use the NH climatology from *Lübken* [1999] as a reference which is tempting because the winter/summer transition in NH stratospheric winds is much more regular compared to the SH.
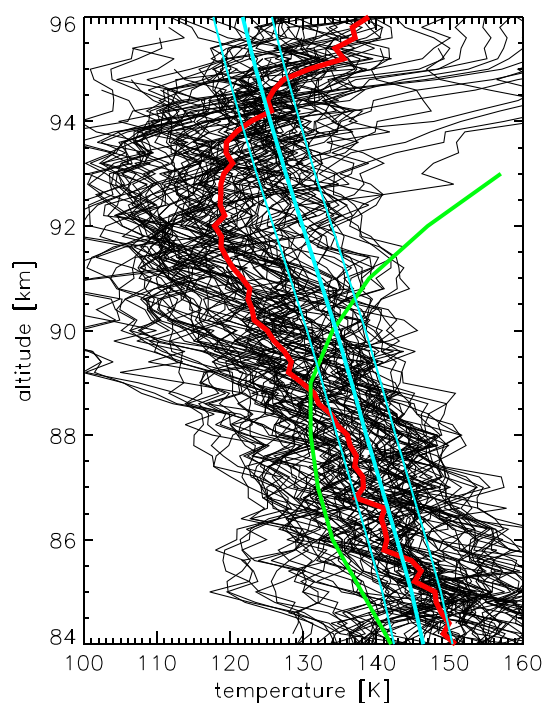
Figure 1. A total of 96 temperature profiles obtained on 17/18 December 2011 (drs = −3/−4). Red line: mean profile; green line: reference profile from the NH for mid-June [from *Lübken*, 1999]; blue lines: frost-point temperatures and variation by ±4 K.

2. Lidar Observations at Davis

The mobile scanning iron lidar is a two-wavelength system (772 nm/386 nm). It determines mesospheric temperatures by probing the Doppler broadened iron resonance line at 386 nm with a frequency-doubled alexandrite laser [*Höffner and Lautenbach*, 2009]. The system allows to measure temperatures during full daylight with a typical uncertainty of less than ±5 K after 1 h integration. These values refer to summer conditions when metal densities are lowest, and the Sun is at its highest elevation. In this study we use a height resolution of 1 km. The iron lidar of the Institute of Atmospheric Physics (IAP) in Kühlungsborn, Germany, was transported to Davis, Antarctica (68.6°S), in November 2010. It performed first measurements on 15 December 2010 and finished operation on 31 December 2012. In total, 2900 h of temperature profiles are now available. Here we concentrate on 736 h of measurements performed during the full summer season of 2011/2012, more precisely from days relative to solstice (drs) = −60 to drs = +60.

In Figure 1 we show 24 h of temperature measurements (96 profiles) on 17/18 December 2011. Occasionally, temperatures are as low 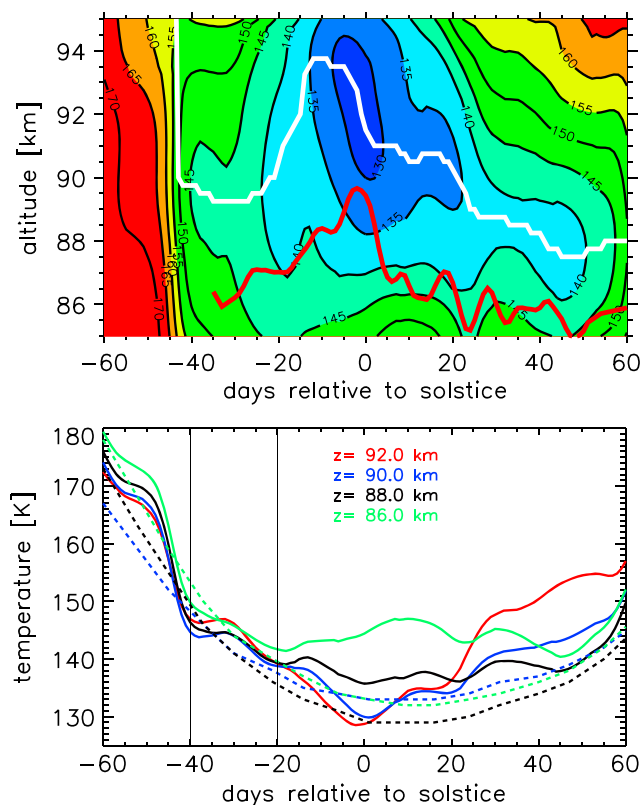as 100 K. The altitude range of reliable temperatures is limited by low iron number densities. Above approximately 95–96 km, Fe density gets low which implies less reliable temperatures and larger uncertainties. From the mean of individual profiles shown in Figure 1, we determine a mesopause altitude and temperature of approximately 92.5±1.5 km and $T = 119±1.3$ K, respectively (the temperature uncertainty is given by counting statistics of the lidar). The root-mean-square variation of temperatures at a fixed altitude is on the order of ±10 K. From the temperature climatology in the Northern Hemisphere at the same latitude (69°N) and in the corresponding time of year (= mid-June), we find a mesopause height and temperature of 88–89 km and 131 K [*Lübken*, 1999], i.e., the mesopause at Davis at the day shown in Figure 1 is significantly higher (by ~4 km) and colder (by ~12 K) compared to the NH reference. Furthermore, at altitudes below approximately 89 km, temperatures over Davis on that day are higher by typically 5–8 K compared to the NH reference. The positive temperature gradient above the mesopause is rather similar in both hemispheres.

We also show frost-point temperatures T_f in Figure 1 where we have used water vapor concentrations from an updated version of the model by *Sonnemann et al.* [2012]. We have added lines by varying T_f by ±4 K to roughly indicate that the actual H_2O profile on that day may have been different from the model profile (note that in the Southern Hemisphere summer mesopause region, a variation of T_f by 4 K corresponds to a change of H_2O concentration by a factor of 4). As can be seen from Figure 1 temperatures are low enough for ice particles to exist ($T < T_f$) up to ~94–95 km. Indeed, PMSE were observed on that day between 86 and 93 km (not shown). Note that at altitudes significantly above 93 km PMSE cannot be created even if charged ice particles are present because increasing kinematic viscosity prevents the generation of small scale fluctuations by neutral air turbulence [*Lübken et al.*, 2009].

In Figure 2 we show the seasonal variation of temperatures around summer solstice smoothed by a 14 days Hanning filter. A total of 736 h of measurements on 62 days contribute to this plot. The distribution of observations is fairly homogeneous; i.e., there are no large data gaps in this period. In particular, 262 h of measurements have been performed during the period of the high and cold mesopause in December. In Figure 2 the altitude of the mesopause (white line) drops from greater heights to the standard NH summer value of ~88 km around drs = −43 (= 8 November), and temperatures drop quickly prior to that day by

Figure 2. (top) Seasonal variation of smoothed lidar temperatures. White line: mesopause altitude; red line: peak height of the PMSE layer. (bottom) Seasonal variation of temperatures at given altitudes (solid lines; see inlet). Northern Hemisphere reference temperatures are shown as dashed lines [from *Lübken, 1999*], except for 92 km (see text for more details).

as much as 20 K per week at nearly all altitudes. In the NH reference the winter/summer mesopause drop occurs around drs = −45, i.e., at a rather similar day compared to 2011/2012 at Davis. We note that the time scale of our smoothing procedure (14 days) is roughly equivalent to the smoothing applied for the NH climatology (see *Lübken* [1999] for more details). For reasons explained later we call the period from drs = −40 to −20 the "onset period." During the onset period in 2011/2012, temperatures at Davis are rather similar to the NH reference. Thereafter and below ∼88 km, they are significantly warmer by ∼5 K. We hesitate to compare with the NH reference above approximately 90–92 km because the falling sphere technique applied for that climatology is somewhat uncertain at these high altitudes [*Lübken*, 1999]. Comparing Figures 1 and 2, it is obvious that smoothed temperatures can deviate significantly from daily means. For example, mesopause temperatures at drs = −4/−3 (17/18 December) in Figure 2 are ∼130 K, significantly warmer compared to Figure 1.

In Figure 2 we also show PMSE peak altitudes. PMSE started very sparsely around drs = −35 (16 November) with a mean height of 86 km. At that altitude and time of year, the frost-point temperature is approximately 135 K which is smaller compared to mean temperatures in that period and altitude (∼145–150 K; see Figure 2). Still, ice particles may exist ($T < T_f$) for shorter periods if we consider a temperature variability of roughly ±10 K d^{-1} and water vapor uncertainties mentioned above. We note that PMSE occur when temperatures drop below the frost point, as expected. For the rest of the season, PMSE nicely follow the general temporal development of the mesopause, i.e., the peak of the PMSE layer is located approximately 3–4 km below the mesopause (see Figure 2). The good agreement between periods when lidar temperatures predict ice particles to exist, i.e., $T < T_f$, and the occurrence of PMSE is an independent confirmation of the reliability of the lidar technique. We note that PMSE and other MLT ice cloud phenomena give only indirect evidence for certain temperatures but cannot provide details about, for example, the height structure around the mesopause. We plan to perform a detailed comparison between temperatures and PMSE in the near future.

In Figure 3 we show mean temperature profiles at three selected times during the season and compare with the NH reference. We picked drs = −2 (rather then drs = 0) since this is in the center of the cold mesopause period around solstice (see Figure 2). At the beginning of the summer season (drs = −30) temperatures at Davis are rather similar compared to the NH (differences are smaller than ±5 K), whereas close to solstice (drs = −2) the mesopause at Davis is much higher and colder compared to the NH reference for several days. This can be seen from the mean temperature profile for the period 17–25 December (drs = −4 to drs = +4) in Figure 3 where the mesopause height and temperature is 92 km and 124 K, respectively, averaging 130 h of observations corresponding to 67% of the time from first switch-on on 17 December until last switch-off on 25 December. Smoothing the temperature field by a 14 days Hanning filter (see above) gives average mesopause temperatures of ∼130 K, similar to the NH. Later in the summer season (drs = +30), temperatures at Davis are higher by typically 10 K compared to the NH reference.
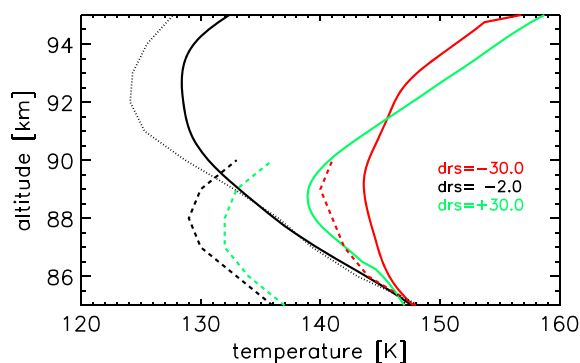
Figure 3. Solid lines: altitude variation of smoothed lidar temperatures at given times (see inlet; drs = days relative to solstice). Dotted line: mean temperature profile from 17 to 25 December 2011 (drs = −4 to +4). Dashed lines: corresponding profiles from the Northern Hemisphere reference [from *Lübken, 1999*] ignoring the uppermost heights (see text for more details).

3. Discussion

We discuss our observations with respect to theoretical expectations presented in *Karlsson et al.* [2011] (hereafter BK11). The main idea is to study stratospheric winds and their impact on mesospheric temperatures [*Smith et al.*, 2010]. Coupling between stratospheric winds and upper mesosphere temperatures comes from gravity waves which are generated in the troposphere and, while propagating upward, are filtered at heights where the phase velocity equals the mean wind velocity. The dissipation of gravity waves deposits momentum, changes vertical winds, and thereby modifies the thermal structure.

BK11 classify stratospheric winds according to a late (early) breakdown of the polar vortex being representative of a "winter-like" (summer-like) condition leading to a high and warm (low and cold) mesopause. "Late" (early) means that zonal winds during the onset-period are higher (lower) by $0.5 \cdot \sigma$ compared to the climatological mean (σ = standard deviation of wind anomalies). If zonal winds develop monotonically with time (as in Figure 2 in BK11), this is equivalent to a late or early breakdown which is defined to occur when the zonal wind at 50 hPa and 65°S gets lower than +10 m/s.

In Figure 4 we show zonal mean zonal winds at 69°S from the MERRA reanalysis at ~50 hPa [*Rienecker et al.*, 2011]. Winds are close to climatology during most of the onset period which would classify this season as being neither late nor early. On the other hand, winds are much larger compared to the climatology from drs ≈ −20 until solstice and the breakdown (u <+10 m/s at 50 hPa) occurs at drs = −1. This would classify the season 2011/2012 as an example of a late breakdown. The situation is obviously more complicated than in BK11. We decided to address the wind situation in the stratosphere as being a quasi-late breakdown.

During the beginning of the onset period we observe the mesopause at standard heights (~88 km) with rather similar temperatures compared to the NH reference (Figure 2). Later in the season, namely, around drs = −20 to +20, the mesopause is higher than the NH reference (90–92 km). Shortly before solstice, the mesopause is highest (93 km) and coldest (119 K). From the discussion in BK11 including the seasonal variation of polar mesospheric clouds (PMC) characteristics, we had expected a higher but warmer(!) mesopause. Relating PMC occurrence to the thermal structure of the summer mesopause is not trivial for
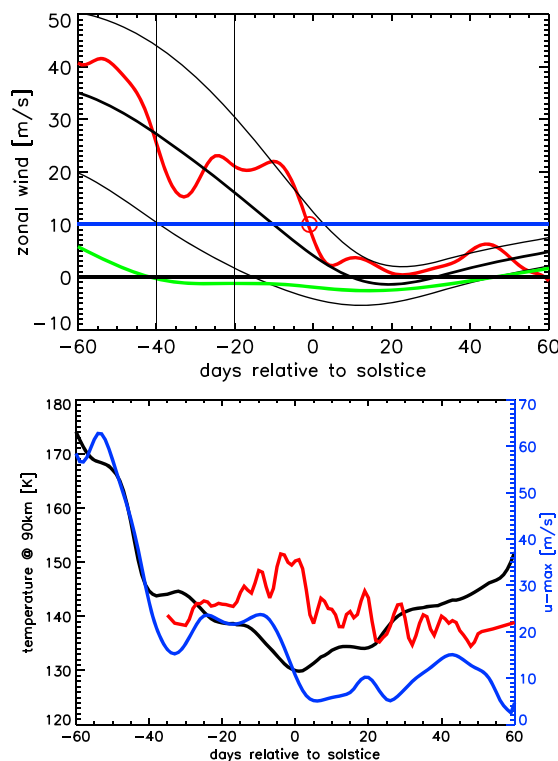
Figure 4. (top) Zonal mean zonal winds at 69°S close to 50 hPa (red line), climatological mean values (thick black line), and standard deviations of wind anomalies (thin black lines). Green line: corresponding mean zonal winds from the NH summer. The horizontal lines mark winds of 0 m/s (for reference) and 10 m/s (the breakdown limit). The two vertical lines mark the onset period (see text). (bottom) Lidar temperatures at 90 km (black) and maximum zonal wind in the stratosphere (blue). Red line: peak height of the PMSE layer.

various reasons. The morphology of PMC discussed in BK11 is a consequence of various factors such as temperatures, water vapor, and circulation. For example, lifting the mesopause altitude from its standard value (88 km) by 5 km (keeping the mesopause temperature and the temperature gradient above and below constant) reduces the amount of water vapor molecules available for ice particle nucleation by roughly a factor of 10 and the visibility of these particles by a factor of 100. The relative importance of water vapor and other factors for the visibility of PMC can only be studied by appropriate models. In this context it is interesting to note that weak and short noctilucent clouds (NLC) were first observed by our lidar on 17 December 2011 (drs = −4), i.e., several weeks after the first appearance of PMSE and significantly later than the winter/summer transition. It is obvious that a SH/NH comparison of PMSE, PMC, and NLC should consider the circulation in the stratosphere. We note that the drop of the mesopause in Figure 4 occurs several days before the onset of the PMSE season. This is because during the winter/summer transition at drs = −43 temperatures in the mesopause region are not low enough to allow for ice particles to exist. In general, the first appearance of PMSE may not coincide with the time of winter/summer transition. This is even more true for PMC and NLC which require ice particles of a sufficiently large size (typically > 20 nm). Obviously, there may be a significant offset between the winter/summer transition in temperatures, the onset of PMSE, and the first appearance of "visible" ice particles (NLC/PMC), respectively. Studies regarding the onset of PMC and its relation to stratospheric circulation changes may therefore be somewhat biased [*Karlsson et al.*, 2011; *Benze et al.*, 2012].

In Figure 4 (bottom) we show the seasonal development of temperatures at 90 km and the maximum zonal wind in the stratosphere, which appear at approximately 10 hPa at drs = −60, declining in altitude to ∼300 hPa after drs = 20. During winter/summer transition in 2011/2012 the maximum wind drops from ∼+60 m/s to ∼+20 m/s within 10 days around drs = −45. As can be seen in Figures 4 and 2, this occurs nearly simultaneously with the steep decline of temperatures at 90 km and the drop of the mesopause. First PMSE appear a few days later. This close correlation between stratospheric winds and MLT temperatures is explained by filtering of gravity waves which are generated in the lower atmosphere [*Smith et al.*, 2010; *Karlsson et al.*, 2011]. Gravity waves with eastward momentum can propagate to the mesosphere only if their phase speed is larger than the maximum zonal wind in the stratosphere. We note that the close correlation between stratospheric winds and temperatures in the mesopause region disappears later in the season, which is presumably due to several factors. For example, the activity of stationary Rossby waves in the winter stratosphere may modify SH mesospheric temperatures, an effect which is known as "interhemispheric coupling" [*Karlsson et al.*, 2009; *Körnich and Becker*, 2010] (note that stationary Rossby wave activity in the NH fully develops only after solstice, i.e., after the winter/summer transition in the SH). Furthermore, the morphology of gravity waves launched in the lower atmosphere may change with season. Other factors such as radiation, chemistry, and turbulence also contribute to the energy budget of the atmosphere and therefore to the seasonal variation of temperatures. More sophisticated modeling is required to study the impact of gravity wave propagation and stratospheric circulation on MLT temperatures.

4. Summary and Conclusions

We have performed quasi-continuous temperature measurements in the SH mesopause region during the winter/summer transition 2011/2012 with high accuracy and high temporal and spatial coverage. Comparison with simultaneous and colocated PMSE observations provides independent confirmation of the seasonal development of low temperatures. We compare the 2011/2012 transition with a NH reference since (i) a suitable climatology is not available for the SH and (ii) winter/summer transitions in the NH stratosphere and mesosphere vary little from year to year, different from the SH. For the winter/summer transition in 2011/2012 we find not only similarities but also significant differences to the NH transition. During the summer season the mesopause is occasionally observed at normal NH values (88 km, 130 K) but also at much higher altitudes ("elevated mesopause"). In the latter case mean mesopause temperatures are typically colder by up to 10 K for several days around solstice. In contrast to mean values, individual temperatures may be as cold as 100 K. We find a good correlation between (i) the time when mesopause heights/temperatures change from winter to summer conditions and (ii) when maximum zonal winds in the stratosphere drop from large to moderate values. After the transition time, the correlation between mesopause heights/temperatures and maximum stratospheric winds is limited. In the future we intend to perform more sophisticated model simulations to better understand the impact of gravity wave sources and propagation through stratospheric winds on the winter/summer transition in the mesopause region

and their impact on NLC, PMC, and PMSE. Unlike in the NH, the SH exhibits significant variability in this transition period and therefore allows to study the relationship between stratospheric dynamics and mesospheric temperatures.

References

Benze, S., C. Randall, B. Karlsson, V. Harvey, M. Deland, G. Thomas, and E. Shettle (2012), On the onset of polar mesospheric cloud seasons as observed by SBUV, *J. Geophys. Res.*, *117*, D07104, doi:10.1029/2011JD017350.

Chu, X., W. Huang, W. Fong, Z. Yu, Z. Wang, J. A. Smith, and C. S. Gardner (2011), First lidar observations of polar mesospheric clouds and Fe temperatures at McMurdo (77.8° S, 166.7° E) Antarctica, *Geophys. Res. Lett.*, *38*, L16810, doi:10.1029/2011GL048373.

Höffner, J., and J. Lautenbach (2009), Daylight measurements of mesopause temperature and vertical wind with the mobile scanning iron lidar, *Opt. Lett.*, *34*, 1351–1353.

Karlsson, B., H. Körnich, and J. Gumbel (2007), Evidence for interhemispheric stratosphere-mesosphere coupling derived from noctilucent cloud properties, *Geophys. Res. Lett.*, *34*, L16806, doi:10.1029/2007GL030282.

Karlsson, B., C. McLandress, and T. G. Shepherd (2009), Inter-hemispheric mesospheric coupling in a comprehensive middle atmosphere model, *J. Atmos. Sol. Terr. Phys.*, 518–530, doi:10.1016/j.jastp.2008.08.006.

Karlsson, B., C. E. Randall, T. G. Shepherd, V. L. Harvey, J. Lumpe, K. Nielsen, S. M. Bailey, M. Hervig, and J. M. Russell III (2011), On the seasonal onset of polar mesospheric clouds and the breakdown of the stratospheric polar vortex in the Southern Hemisphere, *J. Geophys. Res.*, *116*, D18107, doi:10.1029/2011JD015989.

Körnich, H., and E. Becker (2010), A simple model for the interhemispheric coupling of the middle atmosphere circulation, *Adv. Space Res.*, *45*, 661–668, doi:10.1016/j.asr.2009.11.001.

Lübken, F.-J. (1999), Thermal structure of the Arctic summer mesosphere, *J. Geophys. Res.*, *104*, 9135–9149.

Lübken, F.-J., A. Müllemann, and M. J. Jarvis (2004), Temperatures and horizontal winds in the Antarctic summer mesosphere, *J. Geophys. Res.*, *109*, D24112, doi:10.1029/2004JD005133.

Lübken, F.-J., J. Lautenbach, J. Höffner, M. Rapp, and M. Zecha (2009), First continuous temperature measurements within polar mesosphere summer echoes, *J. Atmos. Sol. Terr. Phys.*, 453–463, doi:10.1016/j.jastp.2008.06.001.

Lübken, F.-J., J. Höffner, T. P. Viehl, B. Kaifler, and R. J. Morris (2011), First measurements of thermal tides in the summer mesopause region at Antarctic latitudes, *Geophys. Res. Lett.*, *38*, L24806, doi:10.1029/2011GL050045.

Morris, R. J., D. J. Murphy, R. A. Vincent, D. A. Holdsworth, A. R. Klekociuk, and I. M. Reid (2006), Characteristics of the wind, temperature and PMSE field above Davis, Antarctica, *J. Atmos. Sol. Terr. Phys.*, *68*(3-5), 418–435, doi:10.1016/j.jastp.2005.04.011.

Morris, R. J., J. Höffner, F.-J. Lübken, T. Viehl, B. Kaifler, and A. K. Klekociuk (2012), Experimental evidence of a stratospheric circulation influence on mesospheric temperatures and ice-particles during the 2010–11 austral summer at 69° S, *J. Atmos. Sol. Terr. Phys.*, 54–61, doi:10.1016/j.jastp.2012.08.007.

Pan, W., and C. S. Gardner (2003), Seasonal variations of the atmospheric temperature structure at South Pole, *J. Geophys. Res.*, *108*(D18), 4564, doi:10.1029/2002JD003217.

Rapp, M., and F.-J. Lübken (2004), Polar mesosphere summer echoes (PMSE): Review of observations and current understanding, *Atmos. Chem. Phys.*, *4*, 2601–2633.

Rienecker, M. M., et al. (2011), MERRA: NASA's modern-era retrospective analysis for research and applications, *J. Clim.*, *24*, 3624–3648, doi:10.1175/JCLI-D-11-00015.1.

Smith, A. K., R. R. Garcia, D. R. Marsh, D. E. Kinnison, and J. H. Richter (2010), Simulations of the response of mesospheric circulation and temperature to the Antarctic ozone hole, *Geophys. Res. Lett.*, *37*, L22803, doi:10.1029/2010GL045255.

Sonnemann, G. R., P. Hartogh, U. Berger, F.-J. Lübken, and M. Grygalashvyly (2012), Anthropogenic effects on the distribution of minor chemical constituents in the mesosphere/lower thermosphere—A model study, *Adv. Space Res.*, *50*, 598–618.